DOI: 10.1002/ejic.201100734

Preparation and Biological Evaluation of Di-Hetero-Organometallic-Containing PNA Bioconjugates

Gilles Gasser,*[a] Sebastian Neumann,[b] Ingo Ott,[c] Michael Seitz,[d] Rolf Heumann,[b] and Nils Metzler-Nolte*[d]

Keywords: Bioorganometallic chemistry / Rhenium / Manganese / Biological activity / Peptide nucleic acids

Two peptide nucleic acid (PNA) oligomers containing two different organometallic moieties, namely derivatives of azidoferrocene (Fc-N_3) and ferrocene carboxylic acid (Fc-COOH) for **PNA5** and derivatives of β-cymantrenoylpropionic acid [Cym-CO$(CH_2)_2$COOH] and the rhenium bisquinoline tricarbonyl complex [Re(BQ-N_3)$(CO)_3$]Br for **PNA6**, have been prepared on a solid support by using two different synthetic methods: Peptide coupling and click chemistry. **PNA5** and **PNA6** were unambiguously characterized by ESI-MS or MALDI-TOF MS and their purity checked by LC–MS. As expected, the bioconjugate **PNA6** presents two broad and strong absorption bands at 1933 and 2032 cm^{-1} in its IR spectrum due to the presence of six metal–carbonyl bonds. It has also been demonstrated that the presence of the Mn complex in **PNA6** did not significantly alter the fluorescence properties of the Re complex in aqueous solution compared with a previously reported Re–PNA bioconjugate (**PNA7**). Photoexcitation of **PNA6** at 350 nm reveals two distinct emission bands at about 434 and 595 nm in aqueous solutions. **PNA6** was successfully electroporated into HeLa cells, as shown by high-resolution continuum-source atomic absorption spectroscopy, which was used to measure the concentrations of both Re and Mn. However, no fluorescence of the Re complex in **PNA6** was observed in living cells, even at a concentration 20 times higher than that previously reported for **PNA7**.

Introduction

Peptide nucleic acids (PNAs) are unnatural nucleic acid analogues.[1,2] In PNAs, the usual phosphate-ribose backbone of DNA/RNA is replaced by a neutral pseudo-peptide backbone made of *N*-(2-aminoethyl)glycine units, which are ligated, through a methylenecarbonyl, to the four nucleobases.[1] PNAs have a multitude of attractive properties, such as high binding affinity for DNA/RNA strands, high chemical stability, resistance to nucleases, great discrimination of single mismatches and fast hybridization. These favourable characteristics have led PNAs to be widely investigated for biosensing purposes,[3,4] as agents in antisense and antigene therapy[5] or to facilitate gene repair.[6] An important topic currently in PNA research is the quest for the facile addition of new functionalities and/or spectroscopic properties to PNA oligomers. Hence, numerous metal complexes have been coupled to PNA oligomers with the aim of tuning their physicochemical properties.[7] Organometallic compounds have been found to have ideal properties for this purpose; they are kinetically stable, usually uncharged, relatively lipophilic and their metal atom is in a low oxidation state. Furthermore, they have great structural variety. These attractive properties have led organometallic compounds to be employed as anticancer or antimalarial agents.[8] Different synthetic methods for attaching organometallic complexes to PNA oligomers have been investigated and, until recently, they were always attached to the *N*-terminal end of the PNA sequence through an amide bond, to the side-chain amino group of *N*-terminal (non-natural) amino acids or to the residue of the glycine α-carbon atom of a modified PNA monomer.[9] To allow more versatility in the preparation of PNA oligomers containing multi-metal complexes we recently proposed an alternative approach. In a manner related to that undertaken, for example, by Achim,[10–13] Balasubramanian,[14] Spiccia[15–17] and Strömberg[18,19] and their co-workers, we envisaged the insertion of modified (metal-containing) PNA monomers into PNAs. In our case, we successfully inserted, by using an automated oligonucleotide synthesizer, an alkyne-containing PNA monomer (Fmoc-1-OH, Figure 1) into any

[a] Institute of Inorganic Chemistry, University of Zurich, Winterthurerstrasse 190, 8057 Zürich, Switzerland
Fax: +41-44-635-6803
E-mail: gilles.gasser@aci.uzh.ch
www.gassergroup.com
[b] Biochemistry II – Molecular Neurobiochemistry, Faculty of Chemistry and Biochemistry, Ruhr-University Bochum, Universitätsstrasse 150, 44801 Bochum, Germany
[c] Institute of Medicinal and Pharmaceutical Chemistry, Technische Universität Braunschweig, Beethovenstrasse 55, 38106 Braunschweig, Germany
[d] Inorganic Chemistry I – Bioinorganic Chemistry, Faculty of Chemistry and Biochemistry, Ruhr-University Bochum, Universitätsstrasse 150, 44801 Bochum, Germany
Fax: +49-234-321-4378
E-mail: nils.metzler-nolte@rub.de
www.chemie.rub.de/ac1
Supporting information for this article is available on the WWW under http://dx.doi.org/10.1002/ejic.201100734.

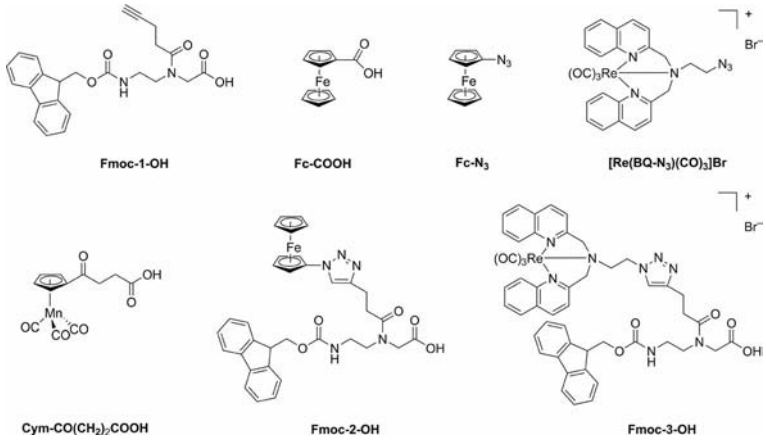

Figure 1. Structures of Fmoc-1-OH and the different organometallic compounds used in this study.

position in a PNA sequence.[20] A similar method has previously been employed by our group to insert a terminal alkyne into peptides for subsequent Sonogashira coupling.[21] The different alkyne-containing PNA oligomers were then quantitatively functionalized on a solid support with ferrocenyl azide (Fc-N_3) by the copper(I)-catalysed Huisgen 1,3-dipolar cycloaddition reaction, often referred to as "click chemistry".[10] However, this method allows the multi-insertion of only one type of organometallic compound. To overcome this limitation, as a proof of principle, we recently investigated the preparation, in solution, of hetero-di-[22] and hetero-tri-organometallic-containing[23] PNA monomers or PNA-like monomers. We demonstrated that three different organometallic compounds could be incorporated into Fmoc-1-OH through three different types of reactions, namely click chemistry, Sonogashira and peptide coupling.[23] In this contribution we further extend this approach by reporting, to the best of our knowledge, the first two examples of the stepwise addition, on a solid support, of two different organometallic complexes to a single PNA oligomer by using two different synthetic methods, namely peptide coupling and click chemistry (Figure 1 summarizes the organometallic compounds used in this work). This "di-organometallic derivatization" of PNA oligomers is of great interest, for example, in multi-modal imaging.[23] Moreover, we employed high-resolution continuum-source atomic absorption spectroscopy (HRCS-AAS) as a novel AAS technique to measure the concentration of both Re and Mn in electroporated HeLa cells.

To show the variety of physicochemical properties that can be added to PNA oligomers through the insertion of organometallic compounds, three different types of these complexes were selected, namely two ferrocene derivatives (Fc-COOH and Fc-N_3), a manganese tricarbonyl complex [β-cymantrenoylpropionic acid, Cym-$CO(CH_2)_2COOH$[24]] and a fluorescent rhenium tricarbonyl compound ([Re(BQ-N_3)$(CO)_3$]Br; Figure 1). The ferrocene derivatives were chosen due to their attractive redox properties and chemical stability;[25,26] Fc-PNA oligomers have already shown great promise in the field of electrochemical PNA·DNA biosensors.[27,28] A tricarbonyl complex [Cym-$CO(CH_2)_2COOH$] was chosen as the second type of organometallic compound to be coupled to PNA oligomers as such complexes have characteristic CO stretching bands, which can be employed to detect, and sometimes quantify, different analytes in biological samples by IR spectroscopy[29] or Raman microscopy.[30] A rhenium tricarbonyl complex ([Re(BQ-N_3)-$(CO)_3$]Br) was selected for its fluorescence properties and potential in radiolabelling studies;[31,32] $[M(CO)_3]^+$ has become a very popular core for radiolabelling experiments, with M = ^{99m}Tc used for radioimaging and M = $^{186/188}$Re for therapeutic applications.[33] Furthermore, Re/Tc tricarbonyl complexes with similar ligands have been shown to have attractive fluorescent/chemical properties, namely large Stokes shifts, long lifetimes, polarized emission, chemical stability and facile preparation, and have already been intensively used for the (radio)labelling of biomolecules by Zubieta, Valliant and Babich and their co-workers for both in vitro and in vivo purposes.[32,34–41] Alberto and co-workers and our group have recently reported the labelling of a PNA monomer and oligomer with Re and ^{99m}Tc tricarbonyl complexes.[42–46]

Results and Discussion

Preparation and Characterization of the Metal-Containing PNA Oligomers

Two different PNA oligomers containing synthon **1** (**PNA1** and **PNA2**) were synthesized on TentaGel R Fmoc-Lys(Boc)-RAM resin using Fmoc-Bhoc-protected PNA monomers (see Scheme 1 for the synthesis of a hetero-di-organometallic-containing PNA oligomer with the preparation of **PNA6** as an example and Table 1 for a summary of the PNA oligomers prepared during the course of this work). The PNA sequence (H-ggg-tc-agc-tt-NH_2) was chosen in analogy to previous work on the derivatization of PNAs with organometallic compounds.[20] Both *C*- and *N*-terminal lysine residues were introduced to enhance the solubility.[47] A small amount of resin was cleaved from both PNA oligomers with a mixture of TFA/triisopropylsilane (TIS)/H_2O (95:2.5:2.5, v/v/v) to determine whether the in-

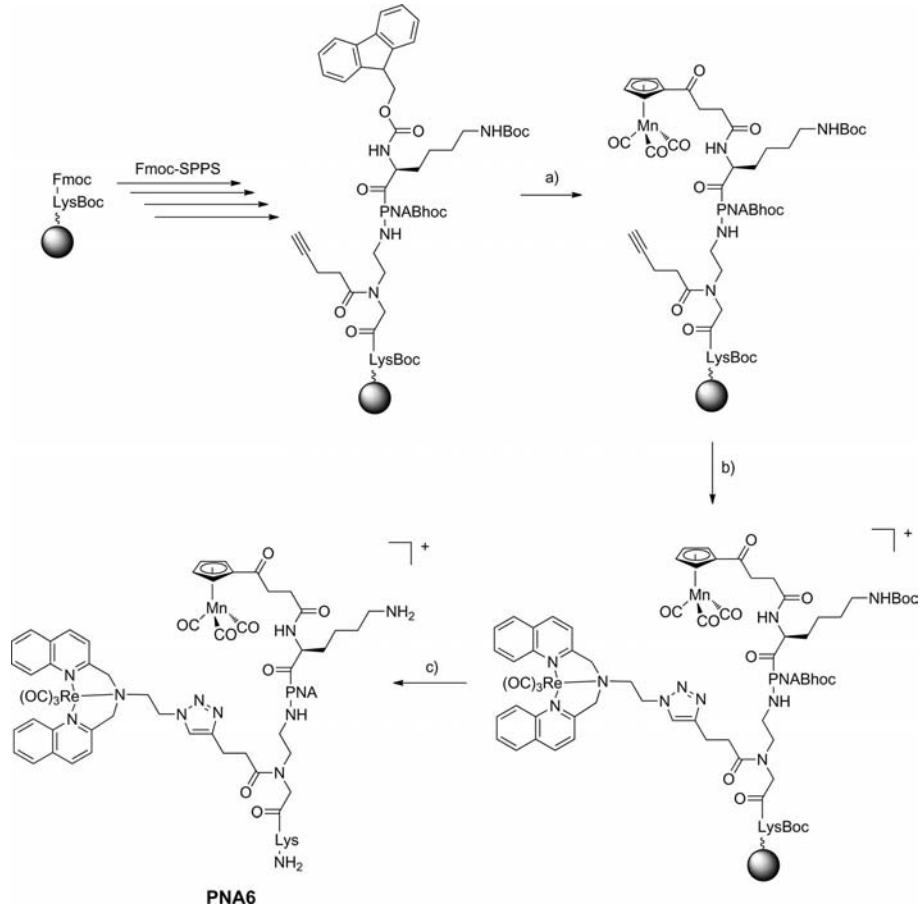

Scheme 1. Synthesis of hetero-di-organometallic-containing PNA oligomer **PNA6**. Reagents and conditions: a) i. 20% Piperidine in DMF; ii. Cym-CO$(CH_2)_2$COOH, HATU, HOBt·H_2O, DIPEA (10 equiv.), 2,6-lutidine (10 equiv.), DMF; b) CuI (2.5 equiv.), [Re(BQ-N_3)$(CO)_3$]-Br (3.0 equiv.), DIPEA (150 equiv.), DMF; c) TFA/phenol/TIS 85:10:5 (v/v/v).

troduction of Fmoc-1-OH was successful. As shown by MALDI-TOF or ESI-MS, Fmoc-1-OH was successfully introduced at the *N* (**PNA1**) and *C* (**PNA2**) termini. Indeed, a peak corresponding to $[M + H]^+$ was observed by MALDI-TOF mass spectrometry for **PNA1** (see Figure S1 in the Supporting Information).[48] Peaks at *m*/*z* = 1597, 1065, 799 and 639 corresponding to $[M + 2H – Fmoc]^{2+}$, $[M + 3H – Fmoc]^{3+}$, $[M + 4H – Fmoc]^{4+}$ and $[M + 5H – Fmoc]^{5+}$ were detected in the ESI-MS spectrum of **PNA2**. The *N*-terminal Fmoc protecting groups of **PNA1** and **PNA2** were then deprotected with a mixture of piperidine in DMF. The newly formed amino terminal groups were subsequently treated, still on the solid support, in a standard peptide coupling procedure, with Fc-COOH and Cym-CO$(CH_2)_2$COOH, respectively, to give the mono-organometallic-containing PNAs **PNA3** and **PNA4**, respectively. A small amount of resin was cleaved from both PNA oligomers with a mixture of TFA/phenol/TIS (85:10:5, v/v/v) to determine whether these coupling reactions were successful. The presence of **PNA3** was ascertained by MALDI-TOF MS with a peak corresponding to $[M + H]^+$ (see Figure S2 in the SI).[48] In the case of **PNA4**, the ESI-MS spectrum clearly shows the presence of the expected oligomer with peaks at *m*/*z* = 1161, 871, 697 and 581 corresponding to $[M + 2H]^{2+}$, $[M + 3H]^{3+}$, $[M + 4H]^{4+}$ and $[M + 5H]^{5+}$, respectively (see Figure S3 in the SI). For both **PNA3** and **PNA4** the last synthetic step involved the copper(I)-catalysed Huisgen 1,3-dipolar cycloaddition reaction. By using reaction conditions similar to those recently reported by our group,[20,49,50] the two alkyne-containing PNA oligomers were functionalized, on the solid support, with Fc-N_3 and [Re(BQ-N_3)$(CO)_3$]Br, respectively, to give the hetero-di-organometallic-containing PNA oligomers **PNA5** and **PNA6**. As for the previous step, a small amount of resin was cleaved from the two PNA oligomers with a mixture of TFA/phenol/TIS (85:10:5, v/v/v) to determine whether the second coupling reactions were successful. Both the success of the click reactions and the purity of the oligomers were analysed by MALDI-TOF and LC–MS. To our surprise, the coupling of the Re complex was found to be almost quantitative. Indeed, the LC chromatogram contains a single major (broad) peak and the three major peaks in the MS at *m*/*z* = 2059, 1373 and 1030 were assigned to $[M + 2H]^{2+}$, $[M + 3H]^{3+}$ and $[M + 4H]^{4+}$, respectively (see Figure S6 in the SI). Note that this broad peak in the LC chromatogram corresponds to a single compound as all the MS spectra recorded at different retention times within this peak are similar (data not shown). This is proba-

bly due to the presence of different PNA conformations in solution, hence the broadening of the peak. Interestingly, the presence of six metal–carbonyl groups in **PNA6** was confirmed by IR spectroscopy with two broad and strong absorption bands at 1933 and 2032 cm^{-1}, respectively (see Figure S6 in the SI). In the case of the di-ferrocene-containing PNA oligomer **PNA5**, both the MALDI-TOF and LC–MS spectra show that the reaction was not fully completed and that a significant amount of the starting material **PNA3** was still present (about 40% by LC–MS). The addition of fresh reagents did not result in any significant improvement, possibly due to steric hindrance. Indeed, compared with **PNA6**, the two organometallic moieties in **PNA5** are in close proximity, thus rendering the cycloaddition more difficult. Nonetheless, both **PNA5** and **PNA6** were cleaved from the resin using a mixture of TFA/phenol/TIS (85:10:5, v/v/v). **PNA5** was purified by HPLC and the expected oligomer was obtained after lyophilization as a fluffy, slightly yellow solid. **PNA5** was unambiguously characterized by ESI-MS with five main peaks at m/z = 1212, 909, 728, 606 and 520 assigned to $[M + 3H]^{3+}$, $[M + 4H]^{4+}$, $[M + 5H]^{5+}$, $[M + 6H]^{6+}$ and $[M + 7H]^{7+}$ and its purity was checked by LC–MS (see Figures S4 and S5 in the SI). The preparation of such di-ferrocene-containing PNAs is of great interest for the sensing of specific DNA/RNA sequences. It can be envisaged that the shift in potential between the two different ferrocenyl moieties could be used to assess the presence or absence of a specific DNA/RNA sequence.

Table 1. **PNA1**–**7** employed during this work. The labels **1**–**3** within the PNA oligomer refer to structures Fmoc-1-OH, Fmoc-2-OH and Fmoc-3-OH presented in Figure 1, respectively.

PNA	Sequences
PNA1	Fmoc-NH-Lys-**1**-ggg-tc-agc-tt-Lys-NH_2
PNA2	Fmoc-NH-Lys-ggg-tc-agc-tt-**1**-Lys-NH_2
PNA3	FcCO-Lys-**1**-ggg-tc-agc-tt-Lys-NH_2
PNA4	Cym-$CO(CH_2)_2CO$-Lys-ggg-tc-agc-tt-**1**-Lys-NH_2
PNA5	FcCO-Lys-**2**-ggg-tc-agc-tt-Lys-NH_2
PNA6	Cym-$CO(CH_2)_2CO$-Lys-ggg-tc-agc-tt-**3**-Lys-NH_2
PNA7	H-Gly-**3**-atgaacttcagggtcagcttgc-Lys-NH_2

Fluorescence Properties of PNA6

To assess whether the presence of a second organometallic entity within a single PNA oligomer could affect the intrinsic fluorescence properties of the Re complex, we studied the photophysical behaviour of **PNA6** in water. As shown in Figure 2, the photophysical data of **PNA6** are comparable to those previously reported by our group for another Re-containing PNA oligomer (**PNA7**, see Table 1).[32,34,37,45] The transitions most likely have considerable metal-to-ligand charge-transfer (MLCT: $[d_\pi(Re) \rightarrow \pi^*(ligand)]$) as well as intraligand (IL) character, in agreement with a previous report.[34] Furthermore, upon photoexcitation at 350 nm, the rhenium complex of **PNA6** shows two distinct emission bands at about 434 and 595 nm in aqueous solution. The high-energy transition has tentatively been assigned to ligand-centred fluorescence, whereas the lower-energy transition probably originates from a ^{3}MLCT state. All in all, the photophysical measurements suggest that **PNA6** could potentially be used as a fluorescent probe in biological settings.

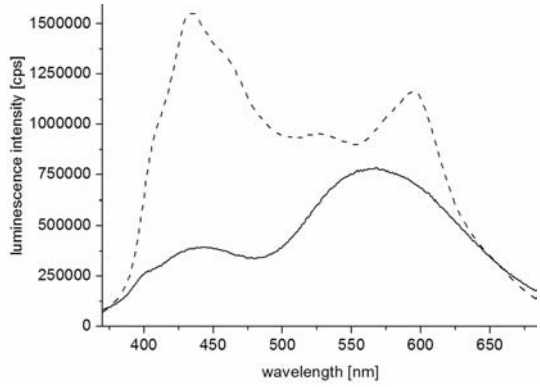

Figure 2. Emission spectra of **PNA6** (dotted line) and **PNA7** (continuous line) in aqueous solution (λ_{exc} = 350 nm, bandwidth: 8 nm) at room temperature.

Biological Evaluation of PNA6

With **PNA6** in hand, we investigated the possibility of using the fluorescence properties of the Re complex to localize the metal–PNA bioconjugate in HeLa cells. Thus, **PNA6** was transfected by electroporation into HeLa cells as previously performed with **PNA7**.[45] The presence of two different metal atoms within a single PNA strand evidently raises questions regarding the toxicity of such bioconjugates. In this study we did not observe any cytotoxic effect of **PNA6** on HeLa cells at concentrations up to 200 μM (data not shown). This observation is in accordance with our previous work, which showed that Co–PNA bioconjugates were not toxic up to a concentration of 100 μM for HT-29 cells.[51] However, to our surprise, we were unable to detect any fluorescence of the Re complex present in **PNA6** in HeLa cells, even at a concentration 20 times higher than that employed to localize **PNA7** in the same cell line.[45] These rather surprising results may be explained by a low cellular uptake of **PNA6**. To confirm/refute such an assumption, we electroporated a concentration of 200 μM of **PNA6** into HeLa cells and measured both the Re and Mn contents of isolated cell pellets after exposure for 24 h. For this purpose we used a novel technique, namely high-resolution continuum-source atomic absorption spectroscopy (HRCS-AAS),[52,53] to quantify sensitive trace metals with simultaneous background correction (for more information on the sensitivity of the method, see the Exp. Sect.). Both Re and Mn could be quantified under the chosen experimental set-up with the absorption signals being well separated from any background interference (see Figure 3 for an example with Mn). In three separate experiments, values of 2.40 ± 0.25 nmol Re and 1.99 ± 0.25 nmol Mn per isolated cell pellet were measured. The Re/Mn ratios of the single experiments afforded a mean ratio of 1.2 ± 0.1. Although it is not definitive evidence, it is reasonable to assume that the

complex is electroporated in an intact (or almost intact) form and that the absence of fluorescence observed for **PNA6** could not be explained by a low cellular uptake of **PNA6**.

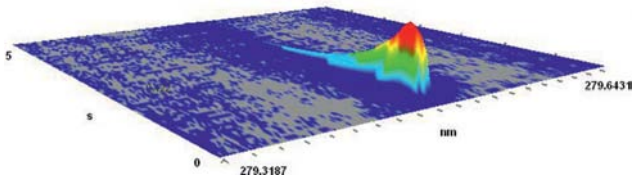

Figure 3. HRCS-AAS measurement of Mn in a cell suspension after electroporation. The figure shows the absorption signal at 279.4817 nm measured over 5 s during atomization.

Conclusions

In this paper we have reported the preparation and characterization of the first two di-hetero-organometallic-containing PNA oligomers (**PNA5** and **PNA6**). Two different types of reactions, namely peptide coupling and copper(I)-catalysed Huisgen 1,3-dipolar cycloaddition (often referred to as "click chemistry"), were employed for the preparation of the two multi-metal–PNA bioconjugates. Interestingly, as shown for the Mn- and Re-containing PNA oligomer (**PNA6**), no cytotoxicity was observed when **PNA6** was electroporated into HeLa cells. The cellular uptake of **PNA6** was confirmed by a novel technique, namely high-resolution continuum-source atomic absorption spectroscopy, which was used to measure the concentrations of both Re and Mn. It was demonstrated that the Re and Mn contents in the HeLa cells were comparable. Although it is not definitive evidence, this is a good indication that a different uptake of possible fragments is of only minor relevance and that the complex is electroporated in an intact (or almost intact) form. However, contrary to our expectations, no fluorescence of the Re complex in **PNA6** could be observed in the electroporated cells, even at a concentration 20 times higher than that employed to localize the previously reported **PNA7** in the same cell line. All in all, this study is further evidence that (multi)-organometallic-containing PNAs can be used for cellular biology purposes, contrary to the general belief that organometallic compounds are unstable under physiological conditions and/or cytotoxic.

Experimental Section

Materials: All reactions were carried out in ordinary glassware and solvents were used without further precautions unless indicated otherwise. Chemicals were purchased from commercial suppliers and used as received. Solvents were used as received or dried with molecular sieves (4 Å).

Instrumentation and Methods: ^{1}H and ^{13}C NMR spectra were recorded in deuteriated solvents with a Bruker DRX 400 spectrometer at 30 °C. Chemical shifts, δ, are reported in ppm (parts per million). Residual solvent peaks were used as internal reference. The abbreviations for the peak multiplicities are as follows: s (singlet), d (doublet), dd (doublet of doublets), t (triplet), q (quartet), m (multiplet) and br. (broad). Infrared spectra were recorded with an ATR unit using a Bruker Tensor 27 FTIR spectrophotometer at a resolution of 4 cm^{-1}. Signal intensity is abbreviated as br (broad) where appropriate. ESI mass spectra were recorded with a Bruker Esquire 6000 spectrometer. All UV/Vis measurements were carried out with a Varian Cary 100 Conc instrument using quartz cuvettes with a width of 1 cm. MALDI-TOF mass spectra were measured with a Bruker Daltonics Autoflex spectrometer. The experiments were performed in linear mode with positive polarity using sinapinic acid as the matrix. **PNA5** was purified by HPLC with a Merck–Hitachi L-7000 instrument equipped with a diode array Uv/vis spectrometer and a Merck LiChroCART RP18 column (5 µm particle size, 100 Å pore size, 250 × 10 mm, flow rate 4 mL/min). The purification was performed with a linear gradient of A (millipore® water containing 0.1% v/v TFA) and B [acetonitrile (Sigma–Aldrich HPLC-grade) containing 0.1% v/v TFA]. Preparative runs: t = 0 min 5% B, t = 12 min 15% B, t = 32 min 40% B, t = 50 min 80% B, t = 51 min 100% B, t = 56 min 100% B, t = 61 min 5% B. LC–MS spectra for **PNA1**–**4** and **PNA6** were measured with a LC Agilent 1100 System equipped with a PDA detector and an auto-sampler using Agilent Zorbax SB-C18 reversed phase columns (1.8 µm particle size). The LC was coupled to a Bruker Esquire 6000 spectrometer to record the mass spectra. The LC runs (flow rate 0.3 mL/min) were performed with a linear gradient of A (Millipore® water containing 0.1% v/v TFA) and B [acetonitrile (Baker HPLC-grade) containing 0.1% v/v TFA]: t = 0 min 0% B, t = 10 min 100% B, t = 12 min 100% B, t = 18 min 0% B, t = 22 min 0% B. The LC–MS spectrum of **PNA5** was measured with an Acquity™ Waters system equipped with a PDA detector and an auto-sampler using a Macherey–Nagel Nucleosil C18 RP column (5 µm particle size, 100 Å pore size, 250 × 3 mm). This LC was coupled to a Bruker Esquire HCT spectrometer (Bremen, Germany) to record the mass spectrum. The LC run (flow rate 0.3 mL/min) was performed with a linear gradient of A (Millipore® water containing 0.1% v/v formic acid) and B [acetonitrile (Sigma–Aldrich HPLC-grade) containing 0.1% v/v formic acid]: t = 0 min 5% B, t = 2 min 5% B, t = 32 min 100% B, t = 37 min 0% B, t = 22 min 0% B.

Synthesis and Characterization

2-[*N*-(2-{[(9*H*-Fluoren-9-yl)methoxy]carbonylamino}ethyl)pent-4-ynamido]acetic Acid (Fmoc-1-OH): Fmoc-1-OH was prepared following the procedure previously published by Gasser et al.[20] The spectroscopic data of the product matched those reported previously.[20]

β-Cymantrenoylpropionic Acid [Cym-CO(CH$_2$)$_2$COOH]: Cym-CO(CH$_2$)$_2$COOH was prepared following the procedure previously published by Schatzschneider and co-workers.[24] The spectroscopic data of the product matched those reported previously.[24]

[Re(BQ-N$_3$)(CO)$_3$]Br: [Re(BQ-N$_3$)(CO)$_3$]Br was prepared following the procedure previously published by Gasser et al.[45] The spectroscopic data of the product matched those reported previously.[45]

PNA7: PNA7 was prepared following the procedure previously published by Gasser et al.[45] The spectroscopic data of the product matched those reported previously.[45]

Synthesis of PNA1 and PNA2: PNA1 was synthesized by using an automated Expedite 8909 nucleic acid synthesizer (Applied Biosystems) adapted for PNA synthesis. The syntheses were performed on a 2-µmol scale with Tentagel R Ram-Lys(Boc)Fmoc resin (0.20 mmol/g) from Rapp Polymer using Fmoc/Bhoc-protected monomers from commercial suppliers (all from Link Technologies, Lanarkshire, Scotland). Synthon Fmoc-1-OH, dissolved in *N*-

methylpyrrolidone (NMP), was inserted into one of the free positions of the synthesizer and a double coupling was applied to ensure full coupling. The SPPS of **PNA2** was performed manually in 5-mL polypropylene one-way syringes as reaction vessels, which were equipped with a frit at the bottom. They were filled with 125 mg of polystyrene resin beads TentaGel R RAM Lys(Boc)-Fmoc (0.20 mmol/g). The resin was swollen in DMF for 1 h before use. All reactions were performed on a mechanical shaker at 400 rpm with approximately 3–4 mL of freshly prepared solutions in the syringes. Fmoc/Bhoc-protected PNA monomers or the Fmoc spacer (5.0 equiv., all from Link Technologies, Lanarkshire, Scotland) were preactivated in Eppendorf tubes before every coupling step for 2 min with HATU (4.5 equiv.) in DMF, adding DIPEA and 2,6-lutidine (10.0 equiv. each) [A(bhoc)-PNA-monomer: 5 min, C(bhoc)-PNA-monomer: 7 min]. For each coupling step the resin beads were treated with the activated acid under vibration and subsequently washed with DMF. The coupling step was monitored by the Kaiser test. Two Fmoc deprotection steps were performed with piperidine (20%, v/v) in DMF (2 + 10 min). The resin beads were then washed successively with DMF, DCM and DMF. The whole procedure (deprotection, coupling, monitoring) was repeated for every PNA monomer until the PNA sequence was completed. Characterization of **PNA1**: MS (MALDI-TOF): *m*/*z* = 3420 $[M + H]^+$.[48] Characterization of **PNA2**: MS (ESI): *m*/*z* = 1597 $[M + 2H - Fmoc]^{2+}$, 1065 $[M + 3H - Fmoc]^{3+}$, 799 $[M + 4H - Fmoc]^{4+}$, 639 $[M + 5H - Fmoc]^{5+}$.

General Procedure for the Cleavage of the PNA from the Resin: Before cleavage, the resin containing the PNA was shrunk with methanol and dried. The non-organometallic-containing PNAs were cleaved using a mixture of trifluoroacetic acid/water/triisopropylsilane (95:2.5:2.5, v/v/v) whereas the organometallic-containing PNAs were cleaved by using a mixture of trifluoroacetic acid/phenol/triisopropylsilane [85:10:5, v/v/v, 3 × 400 μL, 1 h 30 min each)]. The resulting solutions were first evaporated to dryness before being precipitated with ice-cold diethyl ether. The solids were centrifuged, washed with ice-cold diethyl ether and finally air-dried. The crude oligomers obtained were purified by RP-HPLC (in the case of **PNA5**) and finally characterized by ESI-MS or MALDI-TOF MS.

General Procedure for the Synthesis of PNA3 and PNA4 by Peptide Coupling: The polystyrene resin preloaded with the respective PNA sequence (**PNA1** or **PNA2**) was first swollen in DMF for 1 h before use. The last Fmoc protecting group of the sequence was then cleaved with piperidine (20%, v/v) in DMF (2 + 10 min). The resin beads were then washed successively with DMF, DCM and DMF. Fc-COOH (5.0 equiv.) or Cym-$CO(CH_2)_2COOH$ (5.0 equiv.) was preactivated for 3 min in an Eppendorf tube with HATU and HOBt·H_2O (4.5 equiv. each) in DMF with DIPEA and 2,6-lutidine (10.0 equiv. each). The resin was treated with the activated acid under vibration for 4 h to give **PNA3** and **PNA4**, respectively. The resin was then successively washed with DMF, DCM and DMF. The coupling step was monitored by the Kaiser test. See above for details of the subsequent cleavage of the resin. Characterization of **PNA3**: MS (MALDI-TOF): 3411 $[M + H]^+$.[48] Characterization of **PNA4**: MS (ESI): *m*/*z* = 1161 $[M + 2H]^{2+}$, 871 $[M + 3H]^{3+}$, 697 $[M + 4H]^{4+}$, 581 $[M + 5H]^{5+}$.

General Procedure for the Synthesis of PNA5 and PNA6 by Click Chemistry: The polystyrene resin preloaded with the respective PNA sequence (**PNA3** or **PNA4**) was swollen with DMF for 1 h. Fc-N_3 (3.0 equiv.) or $[Re(CO)_3(L\text{-}N_3)]Br$ (3.0 equiv.) and CuI (2.5 equiv.) were then introduced into the syringe (from the top). Afterwards, a mixture of ethyldiisopropylamine (54 μL) and DMF (400 μL) were aspired up the syringe and the mixture was shaken for 3 d at room temperature in the absence of light and under argon. The resin was then washed successively with DMF (5×), CH_2Cl_2 (5×) and DMF (5×). See above for details of the subsequent cleavage of the resin. Characterization of **PNA5**: HPLC: t_R = 16 min. MS (ESI): *m*/*z* = 909 $[M + 4H]^{4+}$, 728 $[M + 5H]^{5+}$, 606 $[M + 6H]^{6+}$, 520 $[M + 7H]^{7+}$. Characterization of **PNA6**: HPLC: t_R = 7.20 min. MS (ESI): *m*/*z* = 2059 $[M + 2H]^{2+}$, 1373 $[M + 3H]^{3+}$, 1030 $[M + 4H]^{4+}$. IR: $\tilde{\nu}$ = 1933 (C≡O), 2032 (C≡O) cm^{-1}.

Calculation of the Extinction Coefficient of $[Mn(CO)_3(CO(CH_2)_2COOH)]$: The extinction coefficient of the Mn complex in the PNA oligomer was estimated by using Cym-$CO(CH_2)_2COOH$ as a model compound. The absorption of Cym-$CO(CH_2)_2COOH$ in H_2O at 260 nm was measured in the concentration range of 30–350 μM. The gradient of the linear plot of the absorption against concentration allowed the extinction coefficient to be calculated: ε_{260} = 3003 $M^{-1} cm^{-1}$.

Determination of the PNA Concentration: The concentration of **PNA6** was measured by using the absorption at 260 nm with the incremental extinction coefficients of the PNA ($\varepsilon_{PNA,A}$ = 13700 $M^{-1} cm^{-1}$, $\varepsilon_{PNA,G}$ = 11700 $M^{-1} cm^{-1}$, $\varepsilon_{PNA,C}$ = 6600 $M^{-1} cm^{-1}$, $\varepsilon_{PNA,T}$ = 8600 $M^{-1} cm^{-1}$).[2] The extinction coefficient used for the Re complex was previously reported by our group (ε_{260} = 9040 $M^{-1} cm^{-1}$).[45] **PNA6** was dissolved in Milli-Q water and then filtered to produce stock solutions. Small aliquots of these stock solutions were then highly diluted in phosphate buffer (100 mM, pH = 7.4). The measurements were carried out at 80 °C at which temperature the PNA strands are completely destacked.

Fluorescence Measurements: Steady-state emission spectra were recorded with a PTI Quantamaster QM4 spectrofluorimeter[54] using ultra-micro quartz cells (Hellma 105.250-QS). The excitation light source was a 75 W continuous xenon short-arc lamp. Emission spectra were collected at 90° to the excitation beam using a PTI R928 photomultiplier tube (operated at –1000 V) as the detector. Spectral selection was achieved by a single grating monochromator (1200 grooves/mm, blazed at 300 nm for the excitation and at 400 nm for the emission).

Cell Culture: Human cervix epithelial cells (HeLa) were used in all cellular experiments. HeLa cells were cultured in cell culture medium [CCM: Dulbecco's modified Eagle's medium (DMEM) supplemented with 10% fetal calf serum (FCS), 2 mM glutamine, 100 U/mL penicillin, 100 μg/mL streptomycin] in T 75 flasks (Sarstedt, Nümbrecht, Germany) at 37 °C and 10% CO_2. All reagents and media were purchased from PAA, Cölbe, Germany. Every 4–7 days the cells were split by trypsination (2.5 mg/mL Trypsin with 0.02 M EDTA) and subcultivated.

Cell Transfection: **PNA6** was transfected into HeLa cells by electroporation using the Amaxa Cell Line Nucleofactor® Kit R (Lonza Cologne AG, Köln, Germany). The electroporation was carried out according to the manufactures' manual. Briefly, 1×10^6 cells were resuspended in 100 μL of Nucleofector® solution, which was further supplemented with 1, 10, 20, 100 or 200 μM of **PNA6**. The suspension was then transferred into a cuvette and electroporated using the program I-13 of the Nucleofector® device. The transfected cells were transferred into 6 mL of CCM (see above) followed by centrifugation at 80*g* for 5 min. After decanting the supernatant, the cells were then resuspended in fresh CCM (500 μL) to a density of 5×10^5 cells per well for cultivation in 24-well plates (TPP, Trasadingen, Switzerland) or to 1.8×10^6 cells in 10 mL CCM per T 25 flask (Sarstedt, Nümbrecht, Germany) at 37 °C and 10% CO_2. As a control, cells were also electroporated

with sterile distilled water, which does not contain any **PNA6**. For high-resolution continuum-source atomic absorption spectroscopy, cells of a T 25 flask were collected 24 h after electroporation.

High-Resolution Continuum-Source Atomic Absorption Spectroscopy: Cell pellets were suspended in 1.0 mL of distilled water and lysed by ultrasonication. In the case of Mn measurements, the lysates were further diluted as appropriate. Aqueous dilutions of **PNA6** were used for calibration purposes. Prior to measurements, 30 μL of HNO_3 (13%) and Triton-X-100 (1%) were added as modifiers and stabilizers to 300 μL of both standard and sample solutions. Re and Mn were measured by using a contrAA 700 high-resolution atomic absorption spectrometer as outlined in more detail below. Injections were performed in duplicate and the respective mean absorbances were used for further calculations. A negative control experiment was performed using untreated HeLa cells to correct for cellular levels of manganese (in the case of rhenium no cellular levels were detectable). The characteristic concentration, which is the concentration leading to a 1% absorption signal and thus reflects the sensitivity of AAS measurements, was 0.10 μM for Re and 0.005 μM for Mn. Accordingly, both applied methods were sufficiently sensitive.

Set-up for Re Measurements: A volume of 30 μL was injected into a PIN-platform graphite tube and thermally processed in the furnace as indicated in Table S1 (see the Supporting Information). Re was detected at a wavelength of 346.044 nm by recording 68 spectra within 5 s.

Set-up for Mn Measurements: The set-up used was similar to that previously reported by Schatzschneider and co-workers.[55] A volume of 20 μL was injected into a regular graphite tube and thermally processed in the furnace as indicated in Table S2 (see the Supporting Information). Mn was detected at a wavelength of 279.4817 nm by recording 68 spectra in 5 s.

Abbreviations: Bhoc = benzhydryloxycarbonyl, CPP = cell-penetrating peptide, Cym = cymantrene, DIPEA = diisopropylethylamine, Fmoc = fluorenylmethoxycarbonyl, HATU = 2-(1*H*-7-azabenzotriazole-1-yl)-1,1,3,3-tetramethyluronium hexafluorophosphate, SPPS = solid-phase peptide synthesis, TIS = triisopropylsilane.

Supporting Information (see footnote on the first page of this article): MALDI-TOF mass spectra of **PNA1** and **PNA3** (Figures S1 and S2), ESI mass spectrum of **PNA4** (Figure S3), LC–MS spectrum of **PNA5** (Figure S4) and IR spectrum of **PNA6** (Figure S6).

Acknowledgments

This work was financially supported by the Swiss National Science Foundation (SNSF Professorship, PP00P2_133568 and Ambizione Grant, PZ00P2_126404 to G. G.), the Alexander von Humboldt Foundation (fellowship to G. G.), the Research Department of Interfacial Systems Chemistry, the Deutsche Forschungsgemeinschaft (DFG) through the Research Unit "Biological Function of Organometallic Compounds" (FOR 630, www.rub.de/for630), the Fonds der Chemischen Industrie (FCI) (Liebig fellowship to M. S.) and the DFG (Emmy Noether fellowship to M. S.). The authors thank Malay Patra for providing Cym-$CO(CH_2)_2COOH$ as well as Anna M. Sosniak and Jan Dittrich for their help in the measurement of the extinction coefficient of Cym-$CO(CH_2)_2COOH$.

[1] P. E. Nielsen, M. Egholm, R. H. Berg, O. Buchardt, *Science* **1991**, *254*, 1497–1500.
[2] P. E. Nielsen, M. Egholm (Eds.), *Peptide Nucleic Acids, Protocols and Applications*, Horizon Scientific Press, Wymondham, UK, **1999**.
[3] N. Hüsken, M. Gebala, W. Schuhmann, N. Metzler-Nolte, *ChemBioChem* **2010**, *11*, 1754–1761, and references cited therein.
[4] S. Martić, M. Labib, P. O. Shipman, H.-B. Kraatz, *Dalton Trans.* **2011**, *40*, 7264–7290, and references cited therein.
[5] P. E. Nielsen, *Curr. Opin. Struct. Biol.* **1999**, *9*, 353–357, and references cited therein.
[6] P. E. Nielsen, *ChemBioChem* **2010**, *11*, 2073–2076, and references cited therein.
[7] G. Gasser, A. M. Sosniak, N. Metzler-Nolte, *Dalton Trans.* **2011**, *40*, 7061–7076, and references cited therein.
[8] G. Gasser, I. Ott, N. Metzler-Nolte, *J. Med. Chem.* **2011**, *54*, 3–25, and references cited therein.
[9] C. Baldoli, P. Cerea, C. Giannini, E. Licandro, C. Rigamonti, S. Maiorana, *Synlett* **2005**, *13*, 1984–1994.
[10] D.-L. Popescu, T. J. Parolin, C. Achim, *J. Am. Chem. Soc.* **2003**, *125*, 6354–6355.
[11] R. M. Franzini, R. M. Watson, G. K. Patra, R. M. Breece, D. L. Tierney, M. P. Hendrich, C. Achim, *Inorg. Chem.* **2006**, *45*, 9798–9811.
[12] R. M. Franzini, R. M. Watson, D.-L. Popescu, G. K. Patra, C. Achim, *Polym. Prepr.* **2004**, *45*, 337–338.
[13] R. M. Watson, Y. A. Skorik, G. K. Patra, C. Achim, *J. Am. Chem. Soc.* **2005**, *127*, 14628–14639.
[14] A. Whitney, G. Gavory, S. Balasubramanian, *Chem. Commun.* **2003**, 36–37.
[15] G. Gasser, M. J. Belousoff, A. M. Bond, L. Spiccia, *J. Org. Chem.* **2006**, *71*, 7565–7573.
[16] G. Gasser, L. Spiccia, *J. Organomet. Chem.* **2008**, *693*, 2478–2482.
[17] N. Nickita, G. Gasser, A. M. Bond, L. Spiccia, *Eur. J. Inorg. Chem.* **2009**, *14*, 2179–2186.
[18] M. Murtola, D. Ossipov, J. Sandbrink, R. Strömberg, *Nucleosides Nucleotides Nucleic Acids* **2007**, *26*, 1479–1483.
[19] M. Murtola, R. Strömberg, *Org. Biomol. Chem.* **2008**, *20*, 3837–3842.
[20] G. Gasser, N. Hüsken, S. D. Köster, N. Metzler-Nolte, *Chem. Commun.* **2008**, 3675–3677.
[21] U. Hoffmanns, N. Metzler-Nolte, *Bioconjugate Chem.* **2006**, *17*, 204–213.
[22] G. Gasser, O. Brosch, A. Ewers, T. Weyhermüller, N. Metzler-Nolte, *Dalton Trans.* **2009**, 4310–4317.
[23] M. Patra, G. Gasser, D. Bobukhov, K. Merz, A. V. Shtemenko, N. Metzler-Nolte, *Dalton Trans.* **2010**, *39*, 5617–5619.
[24] H. W. Peindy N'Dongo, I. Neundorf, K. Merz, U. Schatzschneider, *J. Inorg. Biochem.* **2008**, *102*, 2114–2119.
[25] J. H. R. Tucker, S. R. Collinson, *Chem. Soc. Rev.* **2002**, *31*, 147–156, and references cited therein.
[26] D. R. van Staveren, N. Metzler-Nolte, *Chem. Rev.* **2004**, *104*, 5931–5985, and references cited therein.
[27] N. Hüsken, G. Gasser, S. D. Köster, N. Metzler-Nolte, *Bioconjugate Chem.* **2009**, *20*, 1578–1586.
[28] N. Hüsken, M. Gębala, F. La Mantia, W. Schuhmann, N. Metzler-Nolte, *Chem. Eur. J.*, DOI: 10.1002/chem.20100376.
[29] M. Salmain, A. Vessières, P. Brossier, I. S. Butler, G. Jaouen, *J. Immunol. Methods* **1992**, *148*, 65–75.
[30] K. Meister, J. Niesel, U. Schatzschneider, N. Metzler-Nolte, D. Schmidt, M. Havenith, *Angew. Chem.* **2010**, *122*, 3382; *Angew. Chem. Int. Ed.* **2010**, *49*, 3310–3312.
[31] R. T. Martin de Rosales, C. Finucane, S. J. Mather, P. J. Blower, *Chem. Commun.* **2009**, 4847–4849.
[32] S. James, K. P. Maresca, J. W. Babich, J. F. Valliant, L. C. Doering, J. Zubieta, *Bioconjugate Chem.* **2006**, *17*, 590–596.
[33] R. Alberto, in: *Bioorganometallics: Biomolecules, Labeling, Medicine* (Ed.: G. Jaouen), Wiley-VCH, Weinheim, Germany, **2006**, pp. 97–124.

[34] L. Wei, J. W. Babich, W. C. Eckelman, J. Zubieta, *Inorg. Chem.* **2005**, *44*, 2198–2209.
[35] K. A. Stephenson, S. R. Banerjee, T. Besanger, O. O. Sogebin, M. K. Levadala, N. McFarlane, J. A. Lemon, D. R. Boreham, K. P. Maresca, J. D. Brennan, J. W. Babich, J. Zubieta, J. F. Valliant, *J. Am. Chem. Soc.* **2004**, *126*, 8598–8599.
[36] P. Schaffer, J. A. Gleave, J. A. Lemon, L. C. Reid, L. K. K. Pacey, T. H. Farncombe, D. R. Boreham, J. Zubieta, J. W. Babich, L. C. Doering, J. F. Valliant, *Nucl. Med. Biol.* **2008**, *35*, 159–169.
[37] S. R. Banerjee, J. W. Babich, J. Zubieta, *Chem. Commun.* **2005**, 1784–1786.
[38] K. A. Stephenson, L. C. Reid, J. Zubieta, J. W. Babich, M.-P. Kung, H. F. Kung, J. F. Valliant, *Bioconjugate Chem.* **2008**, *19*, 1087–1094.
[39] S. James, K. P. Maresca, D. G. Allis, J. F. Valliant, W. Eckelman, J. W. Babich, J. Zubieta, *Bioconjugate Chem.* **2006**, *17*, 579–589.
[40] N. Viola-Villegas, A. E. Rabideau, J. Cesnavicious, J. Zubieta, R. P. Doyle, *ChemMedChem* **2008**, *3*, 1387–1394.
[41] A. F. Armstrong, N. Oakley, S. Parker, P. W. Causey, J. Lemon, A. Capretta, C. Zimmerman, J. Joyal, F. Appoh, J. Zubieta, J. W. Babich, G. Singh, J. F. Valliant, *Chem. Commun.* **2008**, *43*, 5532–5534.
[42] C. Xavier, J. Pak, I. Santos, R. Alberto, *J. Organomet. Chem.* **2007**, *692*, 1332–1339.
[43] C. Xavier, C. Giannini, L. Gano, S. Maiorana, R. Alberto, I. Santos, *J. Biol. Inorg. Chem.* **2008**, *13*, 1335–1344.
[44] G. Gasser, K. Jäger, M. Zenker, R. Bergmann, J. Steinbach, H. Stephan, N. Metzler-Nolte, *J. Inorg. Biochem.* **2010**, *104*, 1133–1140.
[45] G. Gasser, A. Pinto, S. Neumann, A. M. Sosniak, M. Seitz, K. Merz, R. Heumann, N. Metzler-Nolte, *Dalton Trans.* **2012**, DOI: 10.1039/C1DT12114F.
[46] G. Gasser, A. M. Sosniak, A. Leonidova, H. Braband, N. Metzler-Nolte, *Aust. J. Chem.* **2011**, *64*, 265–272.
[47] T. Kersebohm, S. I. Kirin, N. Metzler-Nolte, *Bioorg. Med. Chem. Lett.* **2006**, *16*, 2964–2968.
[48] Note that another peak corresponding to $[M + 19]^+$ was also observed in the MALDI-TOF mass spectrum. We assumed that this peak corresponds to $[M + H_2O + H]^+$. Nonetheless, we used this PNA oligomer without further purification in the next synthetic step. The peak was not present in the corresponding product, which suggests that it is the result of an adduct.
[49] A. Sosniak, G. Gasser, N. Metzler-Nolte, *Org. Biomol. Chem.* **2009**, *7*, 4992–5000.
[50] S. D. Köster, J. Dittrich, G. Gasser, N. Hüsken, I. Hernandez, J. L. Jios, N. Metzler-Nolte, *Organometallics* **2008**, *27*, 6326–6332.
[51] S. I. Kirin, I. Ott, R. Gust, W. Mier, T. Weyhermueller, N. Metzler-Nolte, *Angew. Chem.* **2008**, *120*, 969; *Angew. Chem. Int. Ed.* **2008**, *47*, 955–959.
[52] B. Welz, *Anal. Bioanal. Chem.* **2005**, *381*, 69–71.
[53] M. Resano, E. García-Ruiz, *Anal. Bioanal. Chem.* **2011**, *399*, 323–330.
[54] Photon Technology International Inc., Birmingham, NJ, USA.
[55] J. Niesel, A. Pinto, H. W. Peindy N'Dongo, K. Merz, I. Ott, R. Gust, U. Schatzschneider, *Chem. Commun.* **2008**, 1798–1800.

Received: July 15, 2011
Published Online: November 24, 2011

